Desalination and Water Treatment
www.deswater.com
doi: 10.5004/dwt.2023.29142

281 (2023) 163–175
January

Optimization of operating process was triggered by a saltation of ratio in a full-scale activated sludge system

Yongfeng Hu[a,b], Yongxiang Zhang[a,*], Qi Chu[a], Fan Luo[c], Jinglun Cao[c]

[a]*Faculty of Architecture, Civil and Transportation Engineering, Beijing University of Technology, Beijing 100124, China, Tel. +86-13910821850; emails: yxzhang@bjut.edu.cn (Y. Zhang), huyf@emails.bjut.edu.cn (Y. Hu)*
[b]*BCEG No. 3 Construction Engineering, Ltd., Beijing 100044, China*
[c]*School of Environment and Science, Huazhong University of Science and Technology, Wuhan 430074, China, emails: fl4021@hust.edu.cn (F. Luo), jlcao1230@163.com (J. Cao)*

Received 22 April 2022; Accepted 21 November 2022

ABSTRACT

Chemical additions and energy costs in the wastewater industry are increasing trends in more stringent requirements for effluent quality and electricity rates. A novel ratio of chemical P removal addition to influent total phosphorus (TP) is proposed with an application to optimize operation for saving running costs. For this purpose, we monitored the performance of the process for a consecutive year (2018) and established a dynamic model related to the process. The main process variables included the concentration of influent and effluent quantity, chemical oxygen demand, biochemical oxygen demand, total nitrogen, TP, and dosing chemical additions. The ratio of the average daily effective mass of Fe ($M_{\text{Fe-d}}$) to the average daily mass of influent TP ($\text{TP}_{\text{Inf-Tot-d}}$) was found sharply rise to 3.3 g/g or higher in summer and autumn, whereas it smoothly dropped to about 2.3 g/g in winter and spring. This phenomenon can account for enhanced biological phosphorus removal and upset. The emulating results showed that the proposed indicator can provide a relatively accurate representation of the system dynamics while significantly reducing the chemical additions and energy compared to a model that simulates the entire process without a complicated control system and algorithm.

Keywords: Enhanced biological phosphorus removal; Chemical additions; Aeration; Relevance; Model

1. Introduction

Achieving low P effluent (Eff) levels need to have favorable influent (Inf) raw wastewater characteristics and the effectiveness of enhanced biological phosphorus removal (EBPR) in full-scale wastewater treatment plants (WWTPs) [1]. EBPR significantly depends on the activity of polyphosphate accumulating organisms (PAOs), which grows under switching anaerobic and aerobic (or anoxic) conditions. However, due to the event of EBPR upsets [2–4], many of these EBPR facilities performance inconsistently. Commonly factors reported as primary causes of EBPR upsets include: (1) competition for substrate in anaerobic tanks (e.g., between polyphosphate accumulating organisms (PAOs) and glycogen accumulating organisms, (GAOs), or with other denitrifies if nitrate or nitrite are present); (2) low organic loading rates (OLRs) of the plant (e.g., periods of limited availability of readily biodegradable chemical oxygen demand (COD)); (3) individual or combined effect of selected operational conditions and environmental and environmental factors (e.g., high dissolved oxygen (DO), excessive return activated sludge (RAS) recycle rates, long hydraulic retention times (HRTs) in aerobic tanks and secondary clarifiers, high environmental

* Corresponding author.

temperature (T), and overdosing of metals) [5]. When EBPR upset occurs, more chemical P removal addition is fed to meet effluent discharge limits. Therefore, the predictions of EBPR upset and measures against occurrence are of practical importance in full-scale activated sludge system. Santos et al. [5,6] developed a novel metabolic-activated sludge model (ASM) model as a diagnostic tool to predict EBPR instability in a long-term operation of a full-scale three-stage Phoredox (A^2/O) activated sludge system. However, up to now, the metabolic-ASM was not widely applicable to mitigate EBPR upset for copyright, usage fee, and the ability of on-site staff at WWTPs. Thereby, the simultaneous precipitation of phosphorus via the addition of iron or aluminum salts is a very common process for phosphorus removal worldwide [7]. In addition, while the quantity of dosing chemical P agent accounting for running costs was obtained easily and directly by on-site staff, main indexes of influent and effluent water quality indexes (including COD, biochemical oxygen demand (BOD), total nitrogen (TN), NH_3–N, total phosphorus (TP), T, and pH) are monitored and tested manually by on-site staff required by supervision of the government in Beijing.

Among previous studies conducted within the realm of optimal WWTPs, most authors have highlighted different strategies for the optimal operation of WWTPs [8–14]. In addition to the economic aspects, a few reports have discussed other challenges of mitigating EBPR upset. Generally, emerging strategies to improve EBPR stability consist of modifying conventional EBPR configurations with other alternatives. For example, enhancing sludge fermentation to overcome the low availability of readily biodegradable COD in the influent or control of external carbon dosage based on measurements of PO_4^{3-}–P in the effluent or the anaerobic reactor [6]. However, owing to the difficulty of increasing area occupancy and modifying conventional configurations, these measures have been widely questioned, particularly for the existing WWTPs.

The complexity and interconnection of WWTPs hinder the straightforward transition of construction, rehabilitation, management, and operational control. The prior choice for optimizing of existing processes was to enhance process performance with minimal effort. The performance of the side-by-side operation of a conventional anaerobic/anoxic/aerobic (A^2O) process vs. a side-stream enhanced biological phosphorus removal (S2EBPR) process was compared by Wang et al. [13]. They found that the S2EBPR configuration showed improved P removal performance and stability than the conventional A^2O configuration, especially when intermittently operating the mixers in the side-stream anaerobic reactor. Side-stream could be an option for enhancing effectiveness of actual full-scale WWTPs, and adjusting aerobic HRTs is another feasible alternative for mitigating the possible EBPR upset. DO concentration is a crucial factor impacting HRTs, directly changing the activity of PAOs and operating costs. At low DO levels, *Accumulibacter* PAOs were shown to have an advantage over competibacter GAOs, as PAOs had a higher oxygen affinity and thus largely maintained their aerobic activity at low DO levels [15]. Further, an increase in aerobic HRT promoted the proliferation of GAOs over PAOs, decreasing the EBPR efficiency, where DO-based aeration control aimed to maintain a stable DO concentration in biological tanks (at a DO level of 2 mg/L). Attention has also been attracted to simulations and experimental validations aiming to lessen energy consumption and improve nutrient removal performance [16]. Sun et al. [17] concluded that the aeration flow rate was reduced by 20% through the ammonia nitrogen (NH_3–N) and total nitrogen (TN) based on the dynamic aeration control strategy. The study installed in-site NH_3–N and DO probes in the aerobic pool. The aeration control strategy took the form of a two-step cascaded proportion–integration (PI) feedback algorithm. Nonetheless, TP removal and the effectiveness of EBPR were of no discussion. Accordingly, maintaining DO concentrations at fixed aeration areas during operations could still favor energy wastage at different periods and dynamic influent conditions, namely that aeration was not optimized completely. Model tools of WWTPs are of paramount importance that it predicts a promising result in a different operating scenario in optimizing the operation of WWTPs. The well-known activated sludge model (ASM) is widely used to describe the wastewater treatment process [5–7,18,19], even though the limits of the model exist [20].

The primary goal of this study is to conduct in-depth research on the performance of the process and characteristics of dosing chemical P removal addition variation to optimize the process validated by the ASM2d model. For this purpose, we monitored the performance of the process and quantity of dosing chemical additions during an entire year in a full-scale activated sludge system and set up a model related to the process involved in BioWin software. Overall, in contrast to conventional complex control systems and algorithms in full-scale H reclaimed WWTPs, a triggering indicator based on the ratio of daily chemical P removal addition to daily influent TP lanced to optimize the process has enormous potential with respect to the running costs and EBPR upset in developing countries. This full-scale study also provided realistic data and information which could be used in developing EBPR upset prediction models for full-scale systems.

2. Materials and methods

2.1. Full-scale WWTP

2.1.1. WWTP overview

According to the Beijing Municipal Statistical Yearbook of Water Affairs (2020) [21], reclaimed water reached 12 million m^3 (MCM)/y in 2020, which accounted for 29.5% of total water consumption. This indicated significant gaps between the massive demand for water reuse and sanitation services. As the effluent standard became more stringent in this setting, plenty of reclaimed WWTPs were built up. Because of massive demand for water reuse and the scarcity of land resources, the anaerobic-anoxic-oxic membrane bioreactor (A^2O+MBR) process has been widely applied in China. A typical A^2O+MBR process was implemented in H reclaimed WWTP (39°36′~40°02′ N, 116°32′~116°56′ E, Beijing, China) with an area of about 2,000 ha located at Tongzhou New Town [22]. The facility was built in 2011 and began to run in November 2013. The effluent water quality followed in accordance with the first-level limit B of Beijing municipal local standard

'Comprehensive Discharge Standard for Water Pollutants' (DB11/307-2013) [23].

2.1.2. Design, operation, and monitoring

A schematic of the A²O+MBR process is shown in Fig. 1, which consists of four parallel biological treatment series, eight membrane pools, and sixty-four membrane modules in the system.

It was worth mentioning that valves of Q_2 side-stream were no longer available due to equipment damage, and thus diversion rate was 0 during operation. Each aerating area is comprised of four aeration modules (Figs. 2A, B1, B2, and C), which can be controlled independently according to the characteristics of effluent water or operating conditions. Although the higher RR2 of 400% might benefit pollutant removal, this approach would lead to more energy consumption during operation.

The volumes of the anaerobic pool, anoxic pool, interchangeable pool (A and C), aerobic pool (B1 and B2), and membrane pool were approximately 2,500; 8,900; 2,000; 10,500 and 2,500 m^3, respectively. The membrane operating system was operated in the following way: a filtrate flow rate of 350 L/s, a flux of about 0.0185 m/h, a relaxation interval of 7 min, a relaxation duration of 1 min, membrane aeration in an airflow rate of 28,800 m^3/h, maintenance clean by 300~1,000 ppm effective chlorine weekly and soaking time of 0.5~1 h [24]. The values above were obtained from the design and monitoring literature of the consulting engineers [24], and the on-site operational staff's experience.

2.2. Test and analysis

The main monitored and tested indexes include: COD, BOD, TP, TN, NH_3–N, and quantity of chemical additions. A detailed method implemented in this study refers to the 'Water and Wastewater Monitoring and Analysis Method' [25] issued by the Ministry of Environmental Protection of the People's Republic of China (MEP) in 2002.

Chemical analytical tests of the samples were conducted onsite at the H reclaimed wastewater plant laboratory and sent to a third-party lab each quarter. Temperature (T), dissolved oxygen (DO), pH and oxidation–reduction potential (ORP) were measured by Delta Phase (Beijing) probes. There were studies of Pearson's correlation between chemical additions and operating parameters by SPSS Statistics 26. In this study, the software BioWin was provided by the Department of Municipal Engineering, School of Environmental Science and Engineering, Huazhong University of Science and Technology. The overall proposed framework is summarized in Fig. 3.

2.3. Calculation method

The efficiency of pollution removal (R, %) was calculated by Eq. (1).

$$R(\%) = \frac{\text{Concentration}_{\text{Inf}} - \text{Concentration}_{\text{Eff}}}{\text{Concentration}_{\text{Inf}}} \times 100 \quad (1)$$

The Premoval efficiency of biological activities ($R_{\text{Biological}}$%) and chemical additions ($R_{\text{Chemical additions}}$%) were calculated by Eqs. (2) and (3).

$$R_{\text{Biological}}(\%) = \frac{\text{TP}_{\text{Inf}} - \text{TP}_{\text{Eff in model without chemical additions}}}{\text{TP}_{\text{Inf}}} \times 100 \quad (2)$$

$$R_{\text{Chemical additions}}(\%) = R_{\text{Biological+Chemical additions}}(\%) - R_{\text{Biological}}(\%) \quad (3)$$

The daily flow of influent wastewater ($Q_{\text{Inf-d}}$, m^3/d) was calculated by Eq. (4).

$$Q_{\text{Inf}-d} = \frac{\text{quantity of influent wastewater per month}}{N} \quad (4)$$

The Daily flow of the dosing chemical agent ($Q_{\text{Fe-d}}$, m^3/d) was calculated by Eq. (5).

$$Q_{\text{Fe}-d} = \frac{\text{quantity of dosing chemical agent per month}}{N} \quad (5)$$

The effective daily mass of Fe was calculated by Eq. (6).

$$M_{\text{Fe}-d} = Q_{\text{Fe}-d} \times 10\% \quad (6)$$

The effective mass concentration of Fe was not less than 10%.

The daily concentration of influent $\text{Index}_{\text{Inf-d}}$ was calculated by Eq. (7):

$$\text{Index}_{\text{Inf}-d} = \frac{\sum_{1}^{N} \text{daily concentration of inflent index} \times \text{quantity of daily influent wastewater}}{\text{quantity of influent wastewater per month}} \quad (7)$$

The average daily mass of influent TP was calculated by Eq. (8):

$$TP_{\text{Inf}-\text{Tot}-d} = \frac{\sum_{1}^{N} \text{daily concentration of inflent TP} \times \text{quantity of daily influent wastewater}}{N} \quad (8)$$

N denotes the number of monthly days [Eqs. (4), (5) and (8)].

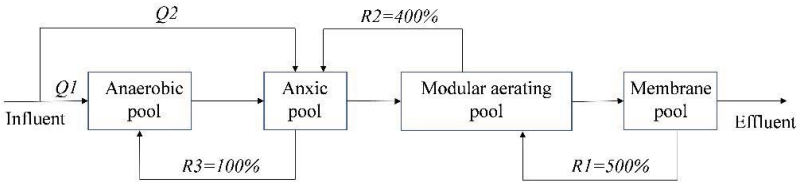

Fig. 1. Schematic diagram of the A²O+MBR process.

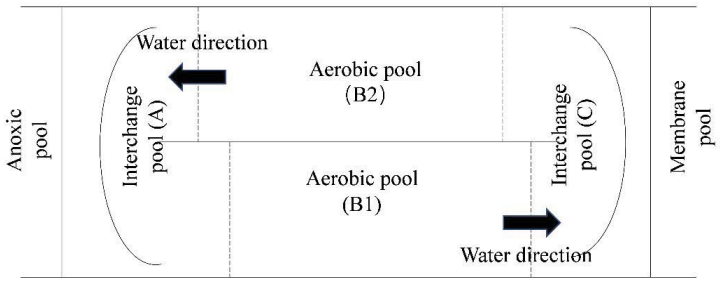

Fig. 2. Schematic of modular aerating areas.

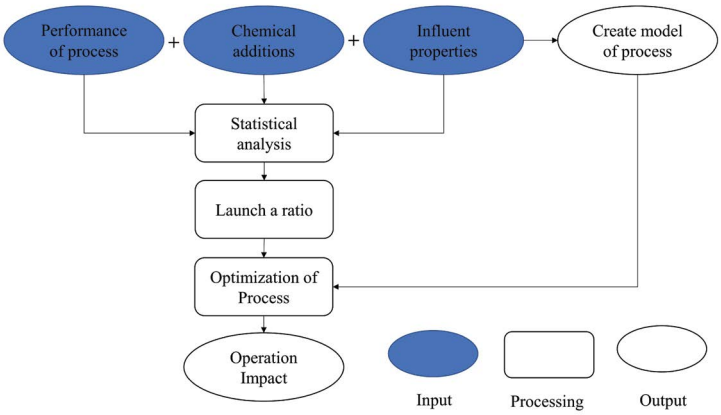

Fig. 3. Proposed framework overview.

2.4. Model study

2.4.1. Model Software

The emulating platform BioWin software based on ASM2d includes 21 biological and chemical reaction processes, with 22 stoichiometric and 45 kinetic parameters [7]. In addition to the biological processes, two chemical processes are used to model chemical P precipitation, as shown in Eq. (9). Further, the absolute values of stoichiometry and kinetics are taken based on the assumption that $Fe(OH)_3$ precipitate S_{PO_4} in the form of $FePO_4$ + $Fe(OH)_3$ [7]. Nevertheless, chemical P precipitation was a very complex process involving various parameters. Mainly depended on chemicals P removal agent and phosphate ion concentrations, supersaturation, ionic strength, temperature, ion types, pH, and time (solid–solid transformation) [26].

$$X_{MeOH} + S_{PO_4} \leftrightarrow X_{MeP} \tag{9}$$

2.4.2. Model established

Only essential components and biochemical processes were included in the model framework to make a succinct model. One series of biochemical reactors was chosen to construct a mode. The model simulation was conducted with calibrated parameters under dynamic state simulation conditions. According to operational conditions, in emulating system (Fig. 4), the temperature (T) of influent water was set at 14°C. The DO set is as follows: anaerobic pool (0 mg/L), anoxic pool (0 mg/L), interchangeable pool (A&C) (2 mg/L), aerobic pool (B1, B2) (2 mg/L). The aeration rate at the MBR membrane pool was controlled at 3,600 m^3/h. Sludge recirculation ratios were set according to operational conditions (Fig. 2). Surplus sludge discharge was approximately 200 m^3/d with the moisture content of 99%. The mass concentration of Fe^{3+} should be at least 10%, and namely mass concentration of $FeCl_3$ should be at least 29.1%. The in-site operating carbon source was NaAc, and 1.0 units of NaAc can be converted to 0.78 units of CH_3 OH in the simulation system. Since the absence of non-degrade substances mixing and the complex testing process, total Kjeldahl nitrogen (TKN) was nearly consistent with TN. Thereby, TN was used in the model instead of total Kjeldahl nitrogen. Although sensitivity analysis of parameters in the model was not the main focus of this study, there was a significant impact of the maximum growth rate, and aerobic decay rate of ammonia oxidation bacteria (AOB), and nitrite oxidation bacteria (NOB) on ammonia simulation output. The maximum growth rate, aerobic decay rate and yield coefficient of heterotrophic bacteria (HB) were also significant on BOD, COD, and TN simulation output [27].

2.4.3. Model calibration

This paper contains properties of influent water quality (Table 1) obtained from former experiments and researchers [22] in the same city, Beijing. As to kinetic and stoichiometric parameters, default values were applied. Parameters of influent fractions were higher than the default values

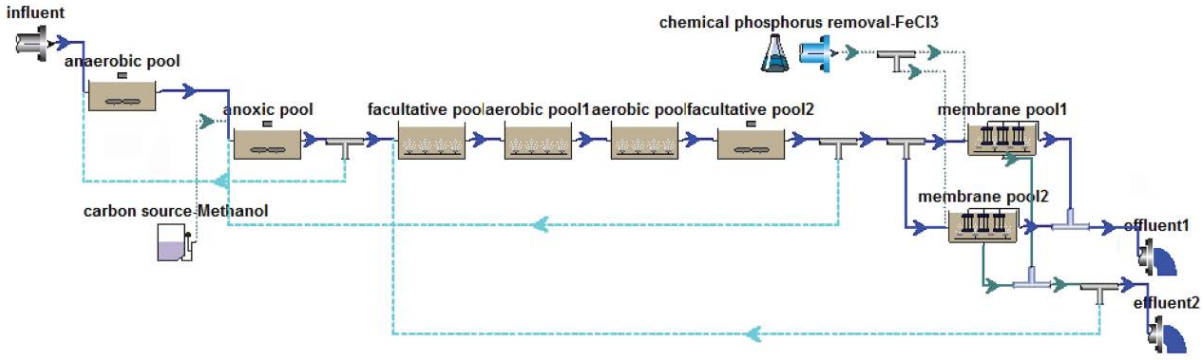

Fig. 4. A²O+MBR process model based on BioWin software.

Table 1
Dynamic state simulation parameters calibration

Parameter	Default value	Calibration value
Percentage of fast-degrading COD[a]	0.160	0.191
Percentage of particulate COD in slow degradation COD[a]	0.750	0.880
Proportion of non-degradable COD in a dissolved state[a]	0.050	0.044
Proportion of non-degradable COD in a particulate form[a]	0.130	0.150
Dissolved biodegradable TKN[a]	0.660	0.752
Alpha factor[b]	–	0.75
Aerobic pool diffuser coverage[c]	%	25.00
Coverage of membrane pool diffuser[c]	%	30.00

[a]Parameters were calibrated around values obtained from former research, and local experiments of influent characteristics of WWTPs in the same city, Beijing [22].
[b]Parameter was calibrated according to an oxygen-transfer experiment by reported Sun et al. [17].
[c]Parameters were calibrated according to the literature [17].

proportion of soluble degradable COD, and TKN due to the difference's location of WWTPs and the living habits of the local people.

2.4.4. Simulation of A²O+MBR process

The fitness of the model to the full-scale A²O+MBR was assessed by comparing the operating data to emulating results (including COD, NH_3–N, TN, and TP).

The average emulating effluent COD, NH_3–N, TN, and TP concentrations were 11.8, 0.66, 11.0, and <0.1 mg/L. Simulating effluent TP concentration was extremely low, resulting from combined EBPR and chemical P removal agent. However, the total chemical P removal agent in the model (126 m^3, effective mass concentration of Fe was not less than 10%) was lower than the actual dosage (150 m^3). This might be caused by side reactions (such as iron salt oxidation precipitation) or avoiding the risk of excess water discharge standards resulting in slight overdosing during operation. There were few reports that a full-scale model of WWTPs in terms of dosing chemical additions, despite ASM2d, was successfully used for describing wastewater process at a pilot scale [28]. The simulated results of COD concentrations (Fig. 5a) were in good agreement with the experimental monitoring. The standard deviation (SD) was 2.53. The fluctuation of the simulation results was less drastic than that of the experiment monitored. The slightly inaccurate simulation may result from the actual parameters of influent fractions variation. The model also showed good fitness in the effluent NH_3–N and TN concentrations. The standard deviation in NH_3–N and TN simulation (Fig. 5b and c) was 0.93 and 0.30, respectively. The average absolute error in COD, NH_3–N, and TN between simulation and actual effluent water quality were 3.3, –0.1, and –1.52 mg/L. Therefore, predictions of the ASM2d model may not be perfect, particularly in terms of actually dosing chemical additions. Overall, the results of the simulation effluent can be accepted, which could provide a relatively liable base for the simulation of the different scenarios.

3. Result and discussion

3.1. Removal efficiency of pollution

The following sections studied the removal efficiency of COD, TN, NH_3–N, TP, and the characteristics of dosing chemical additions in the full-scale activated sludge system.

As explained in Fig. 6a–d, the average removal efficiency of COD, NH_3–N, TN, and TP were 94%, 99%, 77%, and 96%, respectively. Although an indication of fluctuations of removal efficiency existed, the A²O+MBR process was thus prove promising. The average concentration of influent

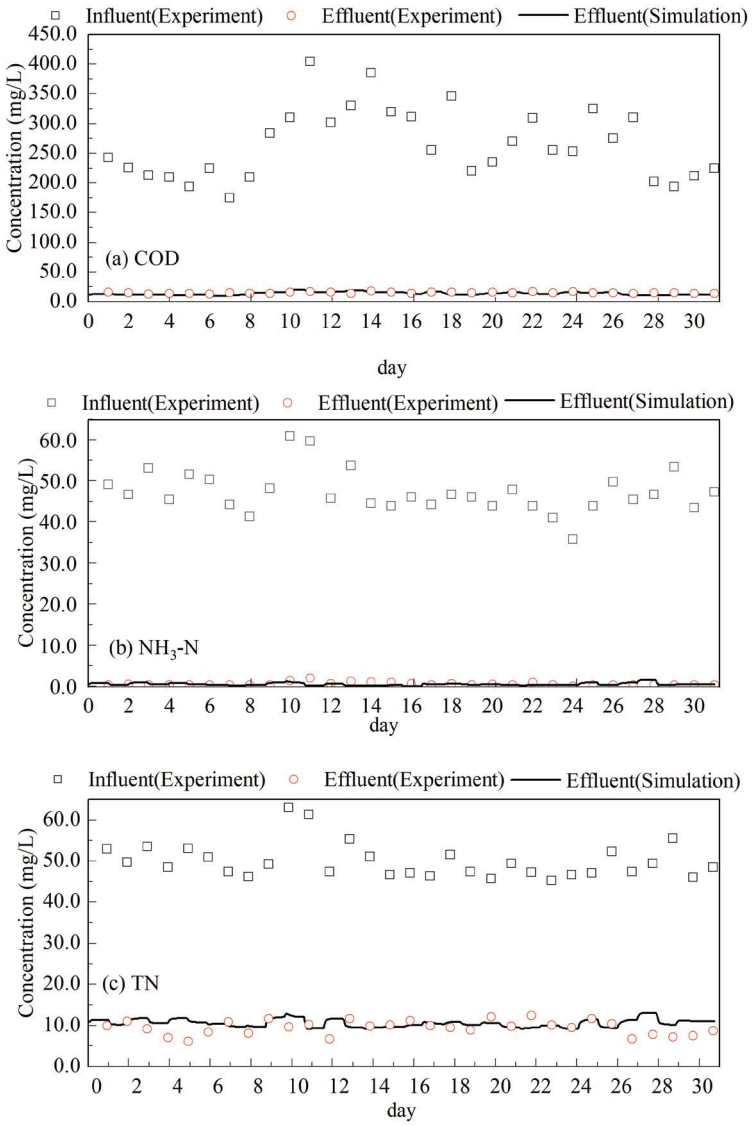

Fig. 5. Influent and effluent of (a) COD, (b) NH_3–N, and (c) TN concentrations compared with the simulation results.

COD in spring and winter was higher than in summer and autumn. This trend was also evident for TN and NH_3–N. The average influent TP concentration was relative stability. The mixing of rainwater could determine this in the sewer network in summer and autumn. Phosphorus release from the sediment could occur in the sewer network.

It should be noted that the concentration of the influent water COD is related to habits and level of living. As the capital, Beijing is one of the most prosperous cities located in the north of China. People lifestyle are different from those in the south of China, such as the frequency of bathing and the style of eating. Thereby, the influent COD concentration in Beijing is higher than in other cities. In comparison, external carbon source addition involves process control ability, mainly determined by on-site staff in the developing countries. External carbon source addition occurs to achieve effluent standards, particularly in low environment temperatures.

3.2. Variation and correlation analysis of chemical additions

The standard deviations were 56.49 and 80.69 per month, while the average daily quantities of Fe ($Q_{Fe\text{-}d}$) and NaAc ($Q_{NaAc\text{-}d}$) were 202.58 and 135.75 m^3, respectively. Table 2 summaries the quantities of influent wastewater ($Q_{Inf\text{-}d}$), dosing chemical P removal agent ($Q_{Fe\text{-}d}$) and external carbon sources ($Q_{NaAc\text{-}d}$) in 2018. Table 3 shows the Pearson's correlation coefficient.

Results suggested that a negative correlation exists between the chemical P removal agent ($Q_{Fe\text{-}d}$) and $BOD_{Inf\text{-}d}$ (Table 4, $r_1 = -0.843$), $BOD_{Inf\text{-}d}$ concentration was lower during summer and autumn than in spring and winter. On account of upgrading groups of MBR modulars, from September average effluent quantity increased to approximately 6,000 m^3/d.

The $M_{Fe\text{-}d}/TP_{Inf\text{-}Tot\text{-}d}$ ratio was 3.3 (g/g) or higher in summer and autumn and was about 2.3 (g/g) (Table 3) in spring and winter. Further, the ratio of $M_{Fe\text{-}d}/TP_{Inf\text{-}Tot\text{-}d}$ in summer

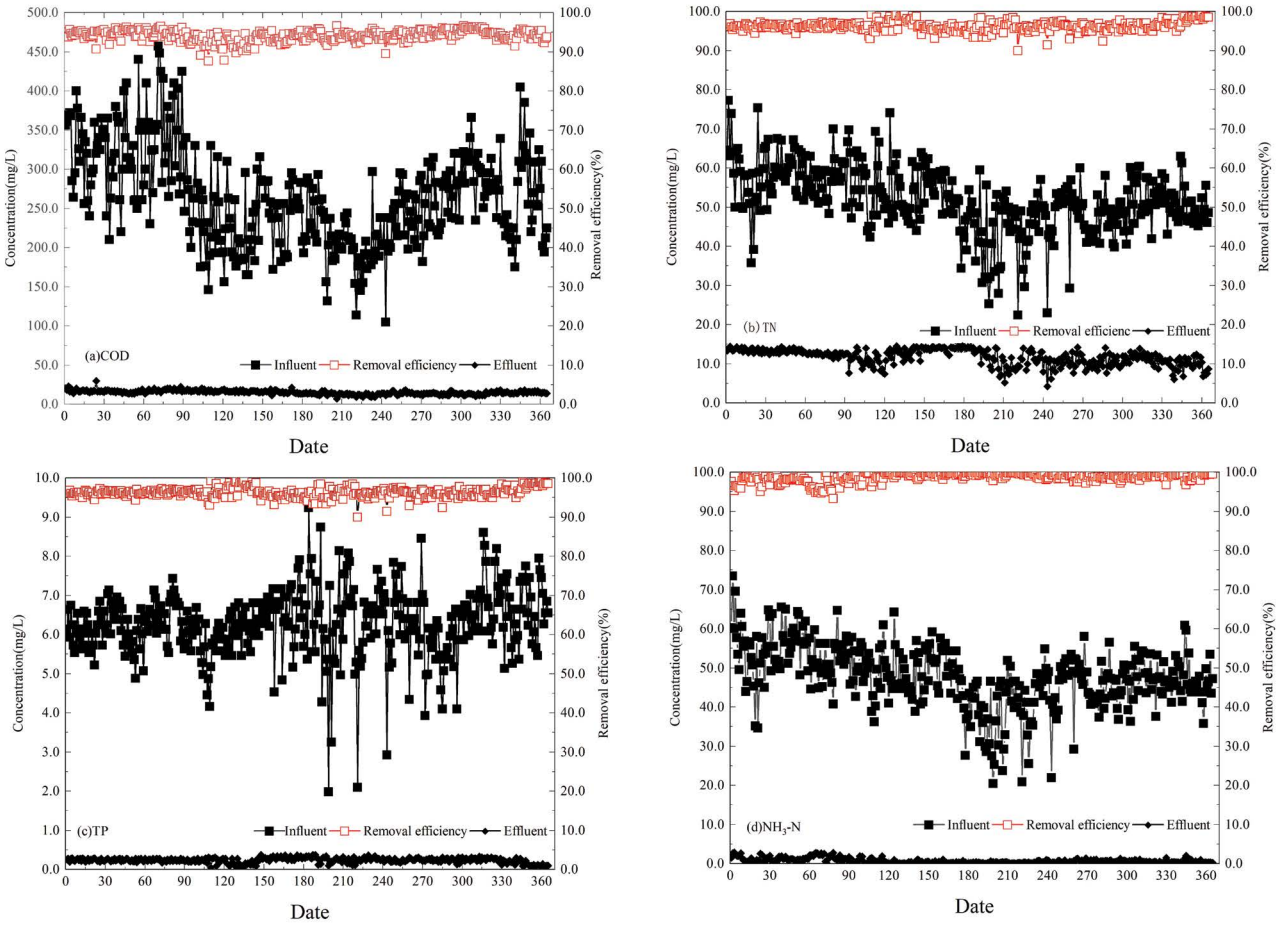

Fig. 6. Removal efficiency of pollution.

Table 2
Main influent characteristics and chemical additions

Month	$Q_{Inf\text{-}d}$ (km^3/d)	$BOD_{Inf\text{-}d}$ (mg/L)	$TP_{Inf\text{-}d}$ (mg/L)	$TN_{Inf\text{-}d}$ (mg/L)	$Q_{Fe\text{-}d}$ (m^3/d)	$M_{Fe\text{-}d}/TP_{Inf\text{-}Tot\text{-}d}$ (g/g)	$Q_{NaAc\text{-}d}$ (m^3/d)
Jan.	31.83	160.52	6.11	57.94	4.52	2.32	1.94
Feb.	31.43	153.68	6.16	59.93	4.57	2.36	2.14
March	30.89	170.00	6.45	57.30	4.52	2.27	1.94
April	33.28	123.68	5.78	55.55	8.53	4.43	2.67
May	35.73	103.15	6.22	53.73	8.81	3.96	2.23
June	33.00	116.00	6.50	52.72	8.10	3.78	2.67
July	31.13	116.31	6.20	43.26	8.94	4.63	3.87
Aug.	31.81	88.42	6.30	44.50	7.74	3.86	4.84
Sept.	37.60	116.84	6.30	49.03	7.80	3.29	8.00
Oct.	38.44	131.05	5.79	46.74	5.81	2.61	7.42
Nov.	37.77	143.68	6.83	52.82	5.67	2.20	7.00
Dec.	37.29	135.26	6.58	49.99	4.84	1.97	8.71

and autumn was of more fluctuations than that in spring and winter. During autumn and winter, a different linear relationship existed between $M_{Fe\text{-}d}/TP_{Inf\text{-}Tot\text{-}d}$ and time-going (Fig. 8, Phase 3), as the same trend occurred in summer (Fig. 8, Phase 2). Nevertheless, it was not sequential and more like a jumping result from the trigger of an EBPR upset, which was strongly affected by high aerobic HRTs, influent OLRs of the plant, and high environmental factors investigated by previous studies [4,5]. Gradually, the performance of EBPR improved to a steady (Fig. 8, Phase 1),

Table 3
Correlation between main influent characteristics and dosing chemical additions

	$Q_{Inf\text{-}d}$ (km^3/d)	$BOD_{Inf\text{-}d}$ (mg/L)	$TP_{Inf\text{-}d}$ (mg/L)	$TN_{Inf\text{-}d}$ (mg/L)	$Q_{Fe\text{-}d}$ (m^3/d)	$M_{Fe\text{-}d}/TP_{Inf\text{-}Tot\text{-}d}$ (g/g)	$Q_{NaAc\text{-}d}$ (km^3/d)
$Q_{Inf\text{-}d}$ (km^3/d)	1	–0.157	0.137	–0.264	–0.012	–0.280	0.808**
$BOD_{Inf\text{-}d}$ (mg/L)		1	0.113	0.683*	–0.843**	–0.748**	–0.188
$TP_{Inf\text{-}d}$ (mg/L)			1	0.007	–0.216	–0.370	0.258
$TN_{Inf\text{-}d}$ (mg/L)				1	–0.497	–0.420	–0.572
$Q_{Fe\text{-}d}$ (m^3/d)					1	0.950**	–0.090
$M_{Fe\text{-}d}/TP_{Inf\text{-}Tot\text{-}d}$ (g/g)						1	–0.297
$Q_{NaAc\text{-}d}$ (km^3/d)							1

*Correlation is significant at the 0.05 level (two-tailed);
**Correlation is significant at the 0.01 level (two-tailed).

Table 4
Simulation conditions

Scenarios	Carbon source	Chemical P removal agent	Q_1	Q_2
1 (C_1)	√	×	*Q*	*0*
2 (C_2)	×	×	*Q*	*0*
3 (C_3)	√	√	*0.7Q*	*0.3Q*

Q was a dynamic influent quantity on each day in Dec. 2018;
0.3*Q* was the max. by-pass side-stream flow to the anoxic pool in the process.

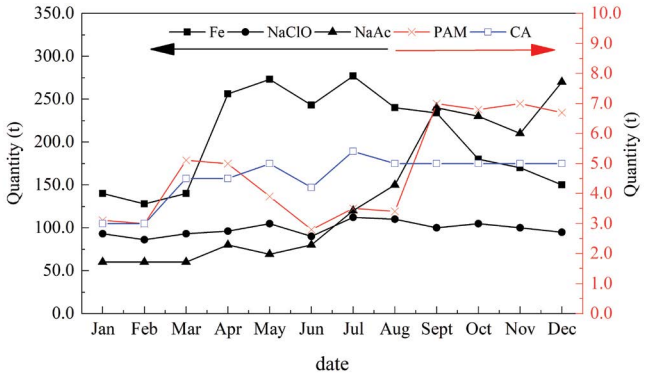

Fig. 7. Chemical additions variation.

leading to less chemical P agent with temperature and influent biodegradable COD/P ratio declining [5]. Due to this characteristic, the process could be optimized with adjusting aeration triggered by the saltation of the $M_{Fe\text{-}d}/TP_{Inf\text{-}Tot\text{-}d}$ ratio. Whereas, if a change in $M_{Fe\text{-}d}$ was caused by fluctuation of effluent TP concentration, adjusting aeration tank modules, in this case, became unnecessary.

Accordingly, the $M_{Fe\text{-}d}/TP_{Inf\text{-}Tot\text{-}d}$ priorities $M_{Fe\text{-}d}$ as a triggering indicator in operation. Additionally, the upset trigger sharply happened 1–2 d before elevated P levels are detectable in the effluent [6]. To overcome the coming EBPR upset, in light of a few factors that can be changed in actual operation, influent OLRs and environmental temperatures were unlikely to be manually changed. As to the H reclaim WWTP, bypass side-stream, HRTs of the aerobic and changing DO concentration in the interchangeable pool (A and C) might be the alternative options, which also be carried out by recent literatures [29,30]. It was essential to monitor the impact of this optimization on effluent qualities simultaneously, especially TN and NH_3–N. These options and effects were discussed in the following sections of this paper. Additionally, Liu et al. [31] suggested that at 10°C the bioactivities of *Tetrasphaera*-dominated communities were obviously inhibited and the EBPR efficiency was only 73%. Yet at 20°C–30°C, EBPR efficiency reached 99% and the relative abundance of *Tetrasphaera* was up to 90%. However, Brown et al. [30] recently reported that in the full-scale activated sludge system abundance of some *Accumulibacter* clades were found contrary some past small-scale studies and studies utilizing synthetic wastewater. Further, abundance of known PAOs did not significantly correlate with changes in phosphorous removal performance, contrary to reports from small-scale and batch studies [31,32]. Thereby, it is worth deeply exploring the differences between small-scale or batch and full-scale studies in terms of microorganisms in the future.

3.3. Discussion of emulating results

The following sections discussed the performance of the process model in different operating and aerating scenarios.

3.3.1. Performance of chemical additions and by-pass side-stream pattern

The related parameters in the scenarios 1 and 2 complied with the sections 2.3.2 and 2.3.3, 'Model established and

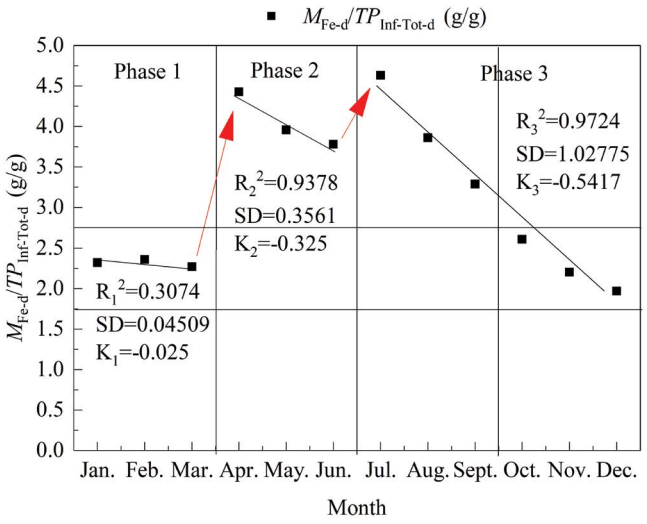

Fig. 8. $M_{Fe-d}/TP_{Inf-Tot-d}$ (g/g) ratio variation in 2018.

Model validation', besides those illustrated in Table 4. Fig. 9 shows the results of the simulation.

The average simulating effluent COD, NH_3–N at scenarios 1, 2, 3 were 15.1, 13.2, 13.56 mg/L and 0.26, 0.29, 0.65 mg/L, respectively. These two indexes achieve the discharge limits. There exist no significant changes in COD and NH_3–N at scenarios 1, 2, 3, and three curves of COD and NH_3–N in Fig. 9a and b fully overlap, and similar trends to TN at scenario 1, 3 (Fig. 9c). Whereas, most of the time, effluent TP discharge limit has not been obtained due to cancelling chemical P removal addition in the ASM2d model in scenarios 1, 2 (Fig. 9d). The average simulated TP concentration of aerobic pool effluent and final effluent were 2.89 and 2.71 mg/L, and the standard deviations were 1.80 and 1.84, respectively. Since that Pearson's correlation coefficient was 1.00, TP at aerobic pool effluent and final effluent (Fig. 8d) have a full correlation. It was again demonstrated that chemical P removal addition coupled with biological phosphorus removal activities plays an important role in the process in term of achieving discharge limits in full-scale WWTPs.

Nevertheless, cancelling chemical P removal addition has little influence on the effluent concentration of TN, which meets the TN discharge limit in scenario 1 (Fig. 9c). In the comparison of simulations C_1 and C_2, it was found that carbon source also profoundly accounts for TN removal. The removal efficiency of TN simultaneously declines, while carbon source is hindered. At the same time, effluent TP concentration decreases immediately. Accordingly, TP removal was promoted, as well as biological TN removal activities with a supplement of carbon source. However, there were more reports that in biological systems, biological N and P removal could form a competitive relationship of carbon source (e.g., volatile fatty acid, VFA) [33,34]. Moreover, a negative correlation exists between biological N and P removal reported by Carvalheira et al. [15].

In scenario 3, the average simulating effluent COD, TN, NH_3–N, and TP concentration (13.65, 0.66, 10.56, and <0.1 mg/L) (Fig. 9a–d) were nearly consistent with the result

Table 5
Simulation conditions

Scenarios	*T* (°C)	DO (mg/L) in the interchangeable pool (A&C)
4 (C_4)	26	2
5 (C_5)	26	0

at section 2.3.4 'Model study: Simulation of A^2O+MBR Process'. The result might suggest that the bypass side-stream slightly improved the removal efficiency of COD, NH_3–N, TN, and TP, which was inconsistent with a previous study [13]. Commonly, in the S2EBPR configuration, both denitrification and EBPR were enhanced. Return activated sludge was diverted into the anaerobic pool to promote fermentation and enrichment of PAOs, and the influent was bypassed to the anoxic pool for enhancing denitrification [13]. For the anaerobic uptake of carbon sources in EBPR systems, GAOs have been shown to compete with PAOs [4]. PAOs had less adaptivity to rapid environmental changes than GAOs, commonly found in temperate EBPR systems and thrived at higher temperatures [35]. In this WWTP, to some extent, P removal was dominated by chemical P removal agents, so the competitive relationship would not be remarkably shown. Overall, external carbon source and chemical P removal were valuable procedure for lower effluent TN and TP concentration. In actual practice, if the TP limit would exceed, there was a preference for dosing chemical P removal agents rather than external carbon sources to promote biological P removal efficiency. Dosing chemical P removal agents produce less residual sludge than carbon sources. Commonly, less sludge means fewer disposal costs. Finally, the carbon source is responsible for about 31% of TN removal and 38.03% of TP removal based on the average simulating values, the chemical P removal addition, and the influent water are responsible for about 39.7% and 20.79% of TP removal.

3.3.2. *Effect of temperature and adjustment of aerating aera*

In the scenarios 4 and 5, operating parameters are shown in Table 5, and the rest complied with sections 2.3.2 and 2.3.3, 'Model Established and Model Validation'. Fig. 10 displays the simulation results.

In scenarios 4 and 5 (Fig. 10a and b), the two curves of COD and NH_3–N partly overlap because of slight differences. In scenario 4, the average simulating effluent NH_3 concentration (Fig. 10b) dropped to about 0.1 mg/L much less than that of the discharge limit. However, the average effluent TN and COD concentration (Fig. 10a and c) were little altered, which were 11.0 and 11.8 mg/L, respectively. Effluent TP concentration (<0.1 mg/L) was still very low without increasing in chemical P removal addition. Simulation results indicated that the temperature increase might be insufficient to produce obvious EBPR upset at high influent BOD concentration. In this case, altering DO concentration at the interchangeable pool (A and C) was the only choice for mitigating possible EBPR upset. In comparing of scenarios 5 with 4, effluent NH_3–N, TN, TP, and COD concentration (Fig. 10a–c) still achieve the discharge limits.

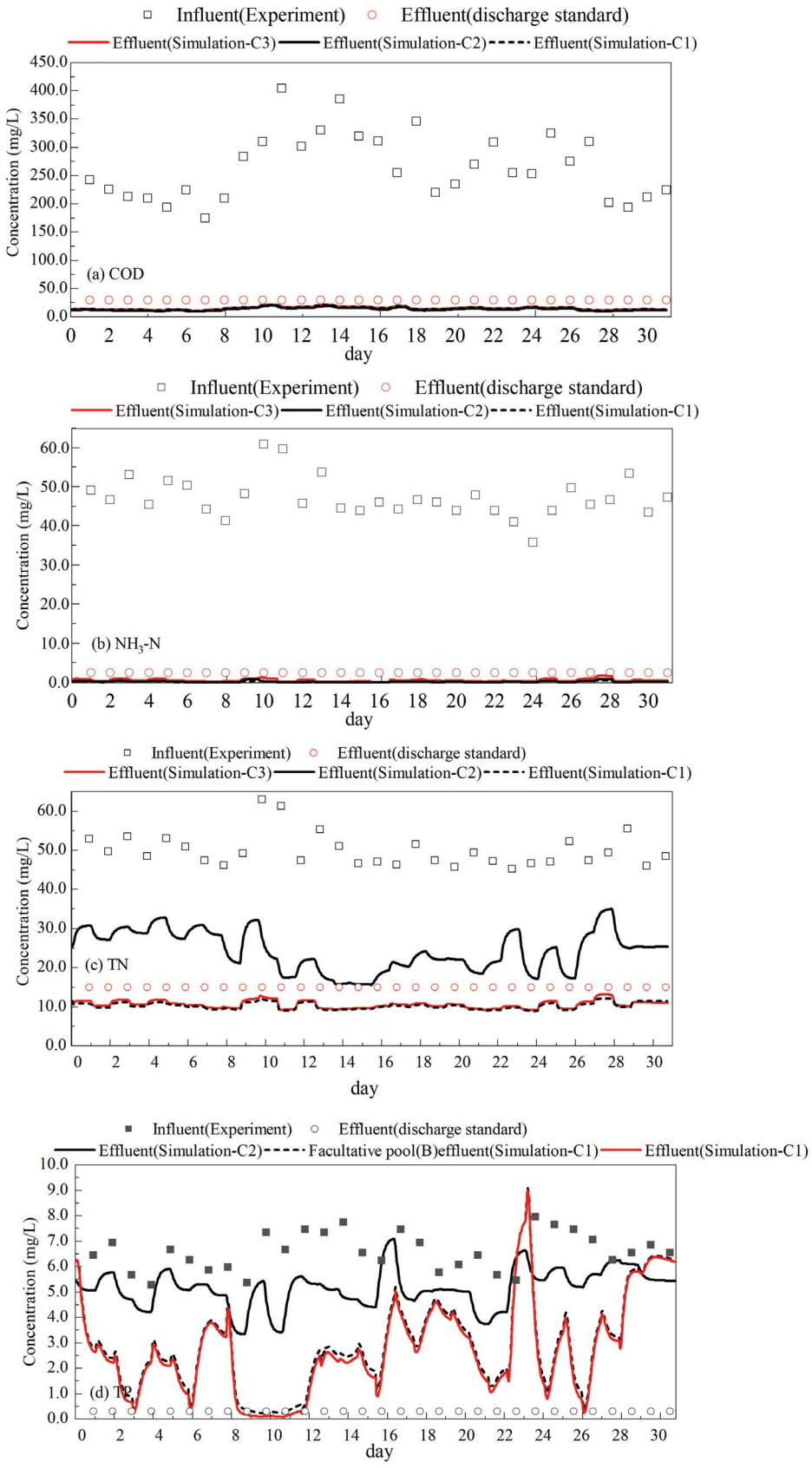

Fig. 9. Simulation results of effluent (a) COD, (b) NH_3–N, (c) TN, and (d) TP concentrations in the scenarios 1, 2, and 3.

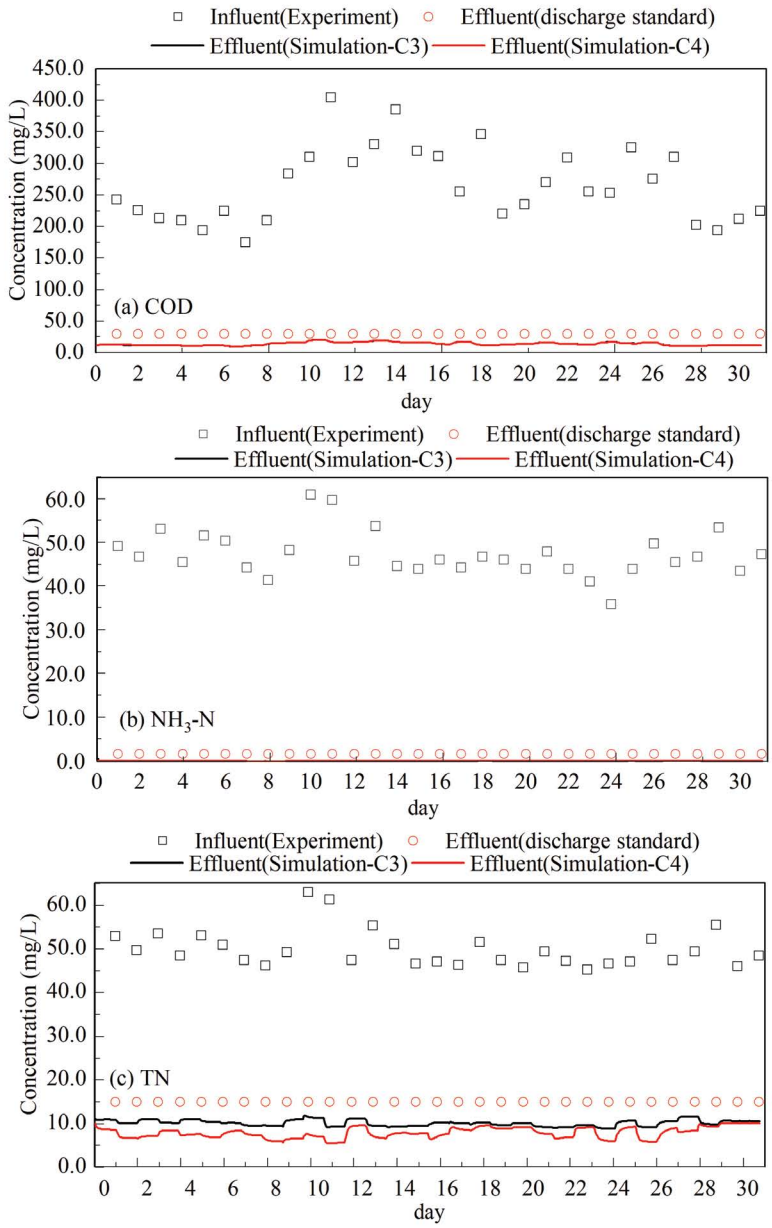

Fig. 10. Simulation results of effluent (a) COD, (b) NH_3–N, and (c) TN concentrations in scenarios 4, 5.

The result matched with the foundation that low HRTs of aeration can be even more beneficial in EBPR performance by selecting for PAOs over GAOs, which could reduce operational costs and improve WWTP sustainability [15]. DO concentration as an operational factor, highly influences EBPR performance and PAOs dominance where high P-removal is achieved at lower DO levels [29]. Accordingly, DO concentration in the interchangeable pool (A and C) could be switched at different operating patterns in different seasons. When the ratio of $M_{Fe\text{-}d}/TP_{Inf\text{-}Tot\text{-}d}$ sharply rose to 3.3 g/g or higher, DO concentration in the interchangeable pool (A and C) was reduced to 0 mg/L in summer and autumn. Aeration in the interchangeable pool (A and C) was switched off, which nearly did not affect the effluent quality, especially COD and NH_3–N, but was a benefit to TN removal. In the H reclaimed WWTP, HRTs ratio of A&C to B1&B2 was 0.4:3.1 lower than 0.15:0.85 reported by Sun et al. [17]. Because of the differences in discharge limits and reducing the risk of exceeding water discharge limits, the gaps can be fully accepted. In winter and spring, as the ratio of $M_{Fe\text{-}d}/TP_{Inf\text{-}Tot\text{-}d}$ dropped to about 2.3 (g/g), aeration in the interchangeable pool (A and C) should be turned on.

4. Conclusion

In this study, the A^2O+MBR process in the full-scale WWTP was proven to be promising. Statistical results showed that a negatively correlation existed between $Q_{Fe\text{-}d}$ and $BOD_{Inf\text{-}d}$ (r = –0.843). Further, the ratio of $M_{Fe\text{-}d}/TP_{Inf\text{-}Tot\text{-}d}$

in summer and autumn was of more fluctuations than that in spring and winter. In the H reclaimed WWTP, if the $M_{Fe\text{-}d}$/$TP_{Inf\text{-}Tot\text{-}d}$ ratio sharply rose to approximately 3.3 g/g or higher in summer and autumn, the time comes to halt aeration at the interchangeable pool (A and C). When it smoothly dropped to 2.3 g/g in winter and spring, it was time to turn on the aeration at the interchangeable pool (A and C). Overall, the ratio of $M_{Fe\text{-}d}/TP_{Inf\text{-}Tot\text{-}d}$ can be regarded as a triggering indicator for optimizing the operational process in full-scale activated sludge systems. While the HRTs ratio of the interchangeable pool (A and C) to the aerobic pool (B1 and B2) was 0.4:3.1, the requirements of discharge limits can be achieved in different seasons. Additionally, chemical P removal addition and the influent water are responsible for about 39.7% and 20.79% of TP removal, while carbon source is responsible for about 31% of TN removal and 38.03% of TP removal based on the average simulating values. As to bypass side-stream, it was of almost no enhancement in the removal efficiency of TN and NH_3–N.

Acknowledgments

This research was funded by integrating and demonstrating technology research and development of Beijing Tianjin Hebei water resources security protection technology (2016YFC0401404). We appreciate this study's technological support from Fan Luo and his institution Department of Municipal Engineering, School of Environmental Science and Engineering, Huazhong University of Science and Technology for this study. We also appreciate the anonymous reviewers' constructive suggestions during the manuscript preparation.

Data availability statement

All data generated or analyzed during this study are included in this published article.

References

[1] P.R. Thomas, D. Allen, D.L. McGregor, Evaluation of combined chemical and biological nutrient removal, Water Sci. Technol., 34 (1996) 285–292.
[2] J. Barnard, D. Houweling, H. Analla, M. Steichen, Saving phosphorus removal at the Henderson NV plant, Water Sci. Technol., 65 (2012) 1318–1322.
[3] J.L. Barnard, M.T. Steichen, Where is biological nutrient removal going now?, Water Sci. Technol., 53 (2006) 155–164.
[4] A. Oehmen, P. Lemos, G. Gcarvalho, Z. Yuan, J. Keller, L. Blackall, M. Reis, Advances in enhanced biological phosphorus removal: from micro to macro scale, Water Res., 41 (2007) 2271–2300.
[5] J.M.M. Santos, A. Martins, S. Barreto, L. Rieger, M. Reis, A. Oehmen, Long-term simulation of a full-scale EBPR plant with a novel metabolic-ASM model and its use as a diagnostic tool, Water Res., 187 (2020) 116398, doi: 10.1016/j.watres.2020.116398.
[6] J.M.M. Santos, L. Rieger, A.B. Lanham, M. Carvalheira, M.A.M. Reis, A. Oehmen, A novel metabolic-ASM model for full-scale biological nutrient removal systems, Water Res., 171 (2020) 115373, doi: 10.1016/j.watres.2019.115373.
[7] M. Henze, W. Gujer, T. Mino, T. Matsuo, M.C. Wentzel, G.V.R. Marais, M.C.M. Van Loosdrecht, M.C.M. Loosdrecht, Activated sludge model No.2d, ASM2d, Water Sci. Technol., 1 (1999) 165–182.
[8] A. Vandekerckhove, W. Moerman, S.W.H. van Hulle, Full-scale modelling of a food industry wastewater treatment plant in view of process upgrade, Chem. Eng. J., 135 (2008) 185–194
[9] M. Vocks, C. Adam, B. Lesjean, R. Gnirss, M. Kraume, Enhanced post-denitrification without addition of an external carbon source in membrane bioreactors, Water Res., 39 (2005) 3360–3368.
[10] W.-J. Liu, Z.-R. Hu, R.L. Walker, P.L. Dold, Enhanced nutrient removal MBR system with chemical addition for low effluent TP, Water Sci. Technol., 6 (2011) 1298–1306.
[11] K. Xiao, Y. Xu, S. Liang, T. Lei, J. Sun, X. Wen, H. Zhang, C. Chen, X. Huang, Engineering application of membrane bioreactor for wastewater treatment in China: current state and future prospect, Front. Environ. Sci. Eng., 8 (2014) 805–819.
[12] J. Guerrero, A. Guisasola, J.A. Baeza, Controlled crude glycerol dosage to prevent EBPR failures in C/N/P removal WWTPs, Chem. Eng. J., 271 (2015) 114–127.
[13] D. Wang, N.B. Tooker, V. Srinivasan, G. Li, L.A. Fernandez, P. Schauer, A. Menniti, C. Maher, C.B. Bott, P. Dombrowski, J.L. Barnard, A. Onnis-Hayden, A.Z. Gu, Side-stream enhanced biological phosphorus removal (S2EBPR) process improves system performance – a full-scale comparative study, Water Res., 167 (2019) 109–115.
[14] B. Xing, M. Ouyang, N. Graham, W. Yu, Enhancement of phosphate adsorption during mineral transformation of natural siderite induced by humic acid: mechanism and application, Chem. Eng. J., 393 (2020) 124–730.
[15] M. Carvalheira, A. Oehmen, G. Carvalho, M. Eusébio, M.A.M. Reis, The impact of aeration on the competition between polyphosphate accumulating organisms and glycogen accumulating organisms, Water Res., 66 (2014) 296–307.
[16] S. Gabarrón, M. Dalmau, J. Porro, I. Rodriguez-Roda, J. Comas, Optimization of full-scale membrane bioreactors for wastewater treatment through a model-based approach, Chem. Eng. J., 267 (2015) 34–42.
[17] J. Sun, P. Liang, X. Yan, K. Zuo, K. Xiao, J. Xia, Y. Qiu, Q. Wu, S. Wu, X. Huang, M. Qi, X. Wen, Reducing aeration energy consumption in a large-scale membrane bioreactor: process simulation and engineering application, Water Res., 93 (2016) 205–213.
[18] B. Ding, X. Zhang, T. Bo, Research on intelligent control system of A/A/O process for wastewater treatment pilot based on ASM2D and fuzzy model, IOP Conf. Ser.: Earth Environ. Sci., 371 (2019) 32060, doi: 10.1088/1755-1315/371/3/032060.
[19] A.C.O. Martins, M.C.A. Silva, A.D. Benetti, Evaluation and optimization of ASM1 parameters using large-scale WWTP monitoring data from a subtropical climate region in Brazil, Water Pract. Technol., 17 (2022) 268–284.
[20] H. Hauduc, L. Rieger, A. Oehmen, M.C.M. van Loosdrecht, Y. Comeau, A. Héduit, P.A. Vanrolleghem, S. Gillot, Critical review of activated sludge modeling state of process knowledge, Biotechnol. Bioeng., 110 (2013) 24–46.
[21] Beijing Municipal Statistical Yearbook of Water Affairs, Beijing Water Authority, 2020.
[22] Z. Xing, Study on the Optimization and Modification of Sewage Treatment Plant Using BioWin Software, Beijing University of Civil Engineering and Architecture, 2016.
[23] Comprehensive Discharge Standard for Water Pollutants (DB11/307–2013), Beijing Municipal Ecology and Environment Bureau, Beijing Municipal Bureau of Market and Quality Supervision, 2013.
[24] L. Yi An, W. Ping, F. Kai, Design and operation of the MBR process at the Hedong Reclaimed Water Plant in Tongzhou, Beijing, Water Wastewater Eng., 44 (2018) 15–17.
[25] Ministry of Environmental Protection China (4th edition), Water and Wastewater Monitoring and Analysis Method, China Environmental Press, 2002.
[26] A. Mañas, B. Biscans, M. Spérandio, Biologically induced phosphorus precipitation in aerobic granular sludge process, Water Res., 45 (2011) 3776–3786.
[27] V.C. Machado, J. Lafuente, J.A. Baeza, Activated sludge model 2d calibration with full-scale WWTP data: comparing

model parameter identifiability with influent and operational uncertainty, Bioprocess. Biosyst. Eng., 7 (2013) 1271–1287.
[28] V.C. Machado, G. Tapia, D. Gabriel, J. Lafuente, J.A. Baeza, Systematic identifiability study based on the fisher information matrix for reducing the number of parameters calibration of an activated sludge model, Environ. Modell. Software, 24 (2009) 1274–1284.
[29] P. Izadi, P. Izadi, A. Eldyasti, Understanding microbial shift of enhanced biological phosphorus removal process (EBPR) under different dissolved oxygen (DO) concentrations and hydraulic retention time (HRTs), Biochem. Eng. J., 166 (2021) 107833, doi: 10.1016/j.bej.2020.107833.
[30] P. Brown, K. Ikuma, S.K. Ong, Biological phosphorus removal and its microbial community in a modified full-scale activated sludge system under dry and wet weather dynamics, Water Res., 217 (2022) 118338, doi: 10.1016/j.watres.2022.118338.
[31] H. Liu, W. Zeng, Q. Meng, Z. Fan, Y. Peng, Phosphorus removal performance, intracellular metabolites and clade-level community structure of *Tetrasphaera*-dominated polyphosphate accumulating organisms at different temperatures, Sci. Total Environ., 842 (2022) 156913, doi: 10.1016/j.scitotenv.2022.156913.
[32] W. Zeng, L. Zhang, P. Fan, Community structures and population dynamics of "*Candidatus accumulibacter*" in activated sludges of wastewater treatment plants using ppk1 as phylogenetic marker, J. Environ. Sci., 67 (2018) 237–248.
[33] T. McCue, R. Naik, M. Zepeda, Y.H. Liu, I. Vassiliev, A.A. Randall, Changes in anoxic denitrification rate resulting from prefermentation of a septic, phosphorus-limited wastewater, Water Environ. Res., 76 (2004) 23–28.
[34] F.J. Rubio-Rincón, C.M. Lopez-Vazquez, L. Welles, M.C.M. van Loosdrecht, D. Brdjanovic, Cooperation between *Candidatus* Competibacter and *Candidatus* Accumulibacter clade I, in denitrification and phosphate removal processes, Water Res., 120 (2017) 156–164.
[35] G. Qiu, R. Zuniga-Montanez, Y. Law, S.S. Thi, T.Q.N. Nguyen, K. Eganathan, X. Liu, P.H. Nielsen, R.B.H. Williams, S. Wuertz, Polyphosphate-accumulating organisms in full-scale tropical wastewater treatment plants use diverse carbon sources, Water Res., 149 (2019) 496–510.